Data impact studies with the AROME WMED reanalysis of the HyMeX SOP1

Nadia Fourrié[1], Mathieu Nuret[1], Pierre Brousseau[1], and Olivier Caumont[1]

[1]CNRM, Université de Toulouse, Météo-France, CNRS, Toulouse, France

Correspondence: Nadia Fourrié (nadia.fourrie@meteo.fr)

Abstract.

This paper presents the results of several observing system experiments (OSEs) performed with AROME-WMED. This model is the HyMeX (Hydrological cycle in the Mediterranean Experiment) dedicated version (Fourrié et al., 2019) of the French operational meso-scale model AROME. The second and final reanalyses assimilated most of all available data for a

5 2 month period corresponding to the first Special Observation Period of HyMeX. In order to assess the impact of various observation data set assimilation on the forecasts, several OSEs or also-called denial experiments, were carried out. In this study, impact of a dense reprocessed network of high quality Global Navigation Satellite System (GNSS) Zenithal Total Delay (ZTD) observations, reprocessed wind-Profilers, lidar-derived vertical profiles of humidity (ground and airborne) and Spanish radar data, is thus discussed.

10 Among the evaluated observations, it is found that the ground-based GNSS ZTD data set provides the largest impact on the analyses and the forecasts as it represents an evenly spread and frequent data set providing information at each analysis time over the AROME-WMED domain. The impact of the reprocessing of GNSS ZTD data also improves the forecast quality but this impact is not statistically significant. The assimilation of the Spanish radar data improves the very short term forecast quality as well as the short term forecasts but this impact remains located over Spain. Marginal impact from wind profilers was

15 observed on wind background quality. No impacts have been found regarding lidar data as they represent a very small data set.

1 Introduction

Heavy precipitation regularly affects the Mediterranean area with huge damages and sometimes casualties. One of the aims of the Hydrological cycle in the Mediterranean Experiment (HyMeX ; Drobinski et al. (2014)) was to study the high impact

20 weather events, especially during the first Special Observation Period one (SOP1,Ducrocq et al. (2014)), which took place in the autumn 2012 (5 September - 6 November 2012) in northwestern Mediterranean. The importance of an accurate description of the low-level humidity flow, which feeds the mesoscale systems, was shown in previous studies (Duffourg and Ducrocq, 2011; Bresson et al., 2012; Ricard et al., 2012). This is why during this period research observations were deployed over the

Natural Hazards
and Earth System
Sciences
Discussions

north-western Mediterranean area. These observations aimed at a better description of the humidity and wind fields. As an

25 example, water vapour lidars were deployed in Candillargues and Menorca island (pink dots in Figure 1). Particular attention was also paid to the control of data quality.

Another important element to better understand the key processes related to the high precipitation and their forecasting is the convective scale modeling. Since many years, such numerical weather prediction models have been implemented in operations to enhance the forecast quality. In addition, the forecast quality depends on their initial atmospheric conditions, which are

30 determined with data assimilation system.

For the HyMeX SOP1 campaign, an AROME (Application of Research to Operations at MEsoscale; (Seity et al., 2011)) version was developed and ran in real-time to forecast and study heavy precipitation in this region: the AROME-WMED (western Mediterranean) model (Fourrié et al., 2015). This model is centered over the western Mediterranean basin and includes a data assimilation system, which provides every 3 hours an analysis of the meteorological situation. In the framework of the

35 Innovative Observing and Data Assimilation Systems for severe weather events in the Mediterranean project, two reanalyses were performed after the campaign (Fourrié et al., 2019) with a view to providing new references for process studies. The first one intended to provide a homogeneous data set of atmospheric fields (which was not the case in real-time version due to a system upgrade in the middle of the SOP1) and the second one included in addition a maximum of observations deployed during SOP1 field campaign with a more recent version of the model. This latter will be considered in this study.

40 Among the research observations assimilated in AROME-WMED reanalysis were the humidity profiles from ground based and airborne lidars. Reprocessing after the campaign was also performed for the wind profiler data (Saïd et al., 2016) and the ground based Global Navigation Satellite System (GNSS) zenithal total delays (ZTD) (Bock et al., 2016) to improve data quality and filter out bad data.

Previous impact studies were already performed for this type of observations in other contexts. For example, Bielli et al.

45 (2012); Grzeschik et al. (2008) tested the impact of the assimilation of water vapour lidars in meso-scale models and found a positive impact of such an assimilation up to the 24-h forecast range. Benjamin et al. (2004) studied the impact of a wind profiler network and obtained a positive impact on short-range (3–12 h) forecasts. Concerning the GNSS data, Mahfouf et al. (2015) showed systematic improvements of the atmospheric humidity short-range forecasts and of the structure and the location of precipitation in the AROME models as found previously in a heavy precipitation context (Boniface et al., 2009). These results

50 agree well with previous studies performed in other NWP models (Macpherson et al., 2008; Gutman et al., 2004)

The aim of the study presented here is to quantify the contribution of the many observation data sets which were assimilated in the AROME-WMED reanalysis of SOP1. To achieve this, a number of denial data assimilation experiments, consisting in removing one observation type, were carried out during the 2-month period of SOP1. The observation data sets considered in this study, are the reprocessed ground based GNSS Zenithal Total Delays (ZTD) observations (Bock et al., 2016), the repro-

55 cessed wind profilers (Saïd et al., 2016), the water vapour profiles from lidar data and the Doppler winds and reflectivities from the Spanish radars. The paper is arranged as follows. Section 2 describes the AROME-WMED configurations and the denial experiments. Section 3 assesses the impact of the ground-based GNSS data assimilation on the analyses and the background during SOP1. Section 4 is dedicated to the impact of GNSS assimilation on the forecast quality. Section 5 provides information

Natural Hazards
and Earth System
Sciences
Discussions

Observations type	amount	percentage
Satellites	8,663,312	53.00%
Surface stations	2,485,620	15.21%
Radars	1,942,539	11.88%
Spanish radars	97,847	0.6%
Aircraft	1,413,313	8.65%
Radiosondes	1,319,523	8.07%
GNSS ZTD	302,191	1.85%
Wind profiler	191,012	1.17%
Lidars	19,470	0.12%
Total	16,346,191	100%

Table 1. Sorted amounts of assimilated data in REANA over the SOP1 period (5 September-5 November 2012).

on the impact of other observation types (i. e. wind profilers, lidars and Spanish radars). Section 6 focusses on the impact of all
these data on the IOP 16a case study. Finally, conclusions are given in Section 7.

2 Sensitivity study description and validation methodology

2.1 AROME-WMED configuration

The different AROME-WMED model configurations are described in Fourrié et al. (2015, 2019) and rely on the operational
limited area model AROME (Seity et al., 2011; Brousseau et al., 2016) version running at Météo-France since 2008. At the
time of the SOP1 campaign, analyses were performed at 2.5 km horizontal resolution every 3 hours with a three dimensional
variational data assimilation (3D-Var, Brousseau et al. (2011)). The AROME-WMED version used in this study as the reference
is the second reanalysis one, named hereafter REANA. An extensive description of the reanalysis can be found in Fourrié et al.
(2019). The main components are recalled here. The model has 60 vertical levels from 10 m above the surface to 1 hPa. Deep
convection is explicitly resolved and one-moment microphysical scheme with five classes of hydrometeors is used (Pinty and
Jabouille, 1998; Caniaux et al., 1994).

Initial atmospheric states of AROME-WMED come every 3 hours from 3D-Var analyses assimilating observations within a
+/- 1h30 assimilation window. The background error statistics were computed over a 15-day period of October 2012 to be more
representative of the meteorological conditions of the SOP1. Lateral boundary conditions are hourly provided by the global
NWP ARPEGE (Courtier et al., 1991) forecasts which benefited from a maximum of assimilated observation with longer
cutoff analyses. Each day at 00UTC, a 54 hour forecast is run. Conventional observations (from radiosondes, aircraft, surface
stations, wind profiler, GNSS ZTDs), radar data and satellite observations (infrared and microwave radiances, atmospheric
motion vectors and ocean surface winds from scatterometers) were assimilated.

Table 1 presents the distribution of assimilated data as a function of observation types. Satellite data represent the majority of observations. This can be explained by the fact that the IASI sensor provides 44 channels per observation point. Surface
80   observations provide 15.21% of assimilated data. Aircraft and radiosondes give similar amount of data (around 8%). GNSS ZTD represent 1.85% of the total and wind profilers 1.17%. Special efforts were made to assimilated non operational data types such as Lidar water vapour profiles and Spanish radar data. Humidity data from Lidar contribute very few with 0.12% of assimilated data. Radar data represent 11.88% of the total amount of assimilated data and Spanish ones only 0.6%.

2.2   Observing System Experiment Description

85   Special efforts were made to assimilate non operational observation data. To study the contribution of the observations on the analysis and forecast quality of the heavy precipitating events of the SOP1, denial experiments have been devised. These experiments consist of removing one observation data set and to compare the forecast quality with and without assimilating this data set. Here, four denial experiments were conducted on the following observation types: the ground-based GNSS ZTD, the wind profilers, the lidar humidity profiles and Spanish radars. The location of these observations is shown in Figure 1.
90   Table 2 summarizes the names of the denial experiments and the observations considered. The largest differences in terms of number of observations are obtained with NOGNSS which leads to a 1.85% difference in the number of assimilated data.

2.2.1   GNSS Zenithal Total delay

We considered here reprocessed data with a homogeneous reprocessing using a single software and more precise satellite orbits position and clocks (Bock et al., 2016), which were available for the whole SOP1. Additional data were also consid-
95   ered compared to the operational and real-time data set. NOGNSS is the experiment without the dense reprocessed GNSS network. Another experiment without re-processed, but with the "operational" GNSS ZTD data assimilated in the real-time AROME-WMED version called OPERGNSS, was also performed to test the impact brought by the reprocessing of the data and additional GNSS data.

2.2.2   Wind profilers

100   These data were available for the whole SOP1 and have been reprocessed after the SOP1 (Saïd et al., 2016) with an improved quality control. Here, observations from 8 wind radars (UHF and VHF) were considered. They are mainly located in the SOuth of France, IN COrsica and Menorca (Figure 1). Experiment without wind profilers is called NOWPROF.

2.2.3   Humidity profiles from Lidars

Experiment without Lidar is NOLIDAR. During SOP1, ground based and airborne lidars were operated. The mobile Water
105   vapour and Aerosol Raman LIdar (WALI, Chazette et al. (2016)) operates with an emitted wavelength of 354.7 nm. This instrument was operated at a site close to Ciutadella (western part of Menorca located by 39 59 07 N and 3 50 13 E). Mixing ratio profiles were delivered with a resolution of 15 m for the 0 m - 6000 m altitude range. A detailed description of this
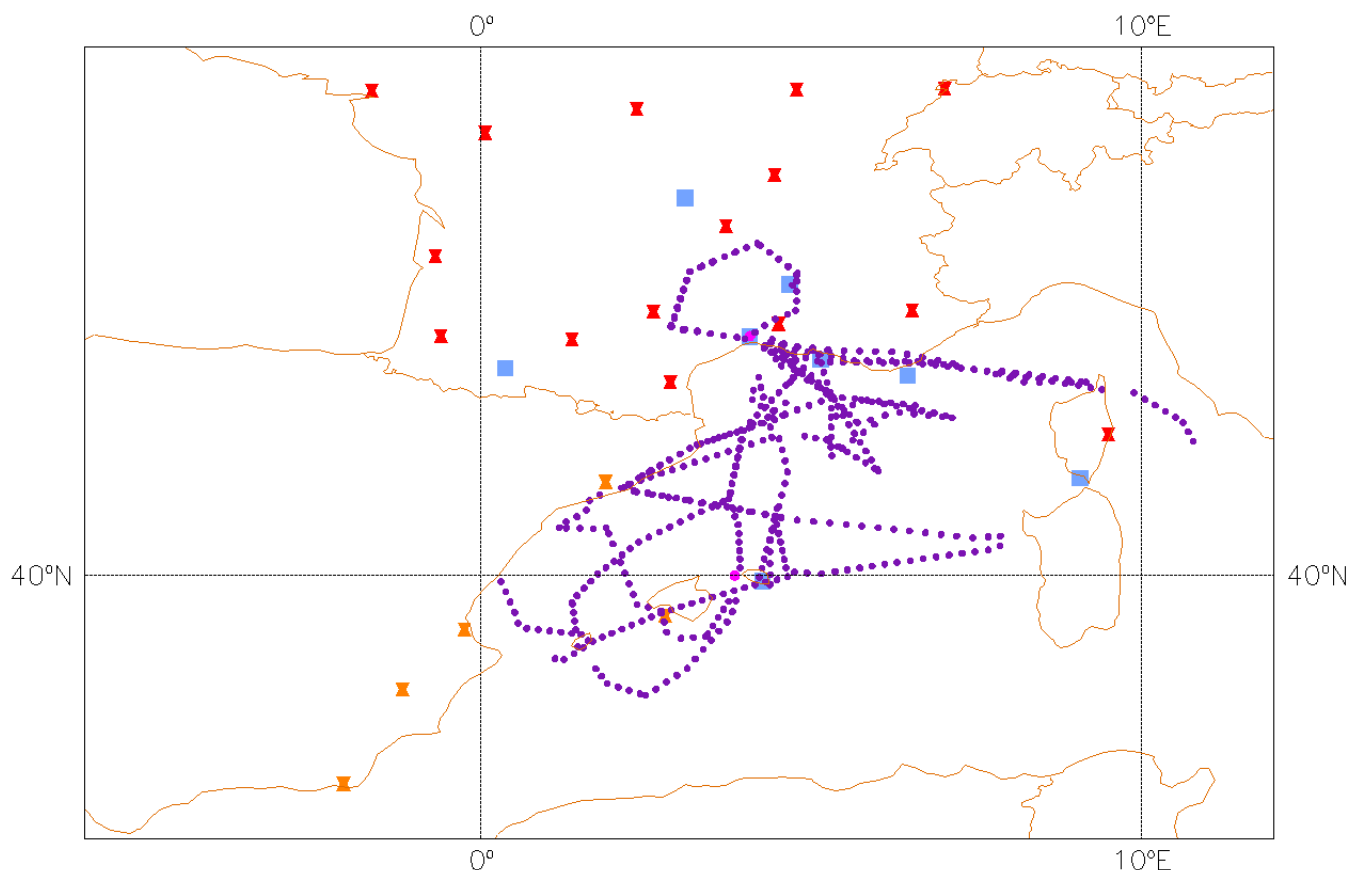
Figure 1. Location of observations considered in this study. Wind profilers are depicted with blue squares, ground based lidars with pink dots, assimilated Leandre II airborne profiles with purple dots, Spanish radars with orange symbols. Red symbols correspond to the French radar locations.

instrument can be found in Chazette et al. (2016). The raw vertical resolution of the data is 75 m but for assimilation, data were thinned at 75 m below 2000 m up to 450 m above 5000 m. The second ground based lidar, the BASIL instrument (Di Girolamo

110 et al., 2016) was located in Candillargues in the South of France. The original resolution is 30 m but data were thinned at 60 m below 1000 m increasing up to 420 m above 4000 m in the assimilation. For WALI, 292 mixing ratio profiles were assimilated in REANA, covering the period 17 September 2012 - 03 UTC to 27 October 2012 - 21 UTC, whereas for BASIL, 172 profiles were assimilated , covering the period 10th September 2012 - 09 UTC to 5th November 2012 15UTC.

Concerning Leandre II lidar (Chazette et al., 2016) on board ATR aircraft, data were available for 22 analysis slots (512

115 assimilated profiles), covering the period 11th September 2012 09UTC to 25 October 2012 21UTC. Profiles with a 150 m vertical resolution were thinned at a 15 km horizontal resolution and are mainly located over the Mediterranean Sea (Figure 1).

2.2.4 Spanish radar data

Doppler radial winds and reflectivities from five Spanish radars (located in Barcelona, Valencia, Almeria, Murcia, Palma de Mallorca) were assimilated in REANA. Only the three lowest elevations have been considered. 10484 observations were thus removed in the NORADSPAIN experiments.

Experiment name	Description	Difference (%) in the number of assimilated data
REANA	AROME-WMED reanalysis (2nd), see Fourrié et al. (2019)	
NOGNSS	REANA - reprocessed GNSS ZTD	-1.86%
OPERGNSS	NOGNSS + operational GNSS ZTD	-1.04%
NOLIDAR	REANA - LIDAR	-0.15%
NOWPROF	REANA - wind profiler	-1.12%
NORADSPAIN	REANA - Spanish radars	-0.6%

Table 2. Description of the data denial experiments discussed in this study and difference (in %) in the number of assimilated data compared to the reanalysis REANA.

2.3 Validation protocol

The evaluation of the various denial experiments is made against the reference REANA run, which includes operational and research observations in its 3D-Var assimilation; all assimilated data are described in a companion paper (Fourrié et al., 2019).

As a first step (Analysis and First-Guess sub-section), the performance of the data assimilation system is evaluated by comparing the various Analyses (AN) and First-Guess (FG) values against the assimilated observation (operational data assimilation monitoring procedure); statistics of departure from observations (mean and Root Mean Square (RMS) error) are computed at the assimilated observation location. Those statistics were also computed using few available independent data. The first source comes from the vessel Marfret-Niolon, which was an instrumented commercial ship of opportunity, cruising regularly between the southern France harbour of Marseille and two Algerian harbours (Algiers and Mostagadem). Please refer to Figure 14 of Fourrié et al. (2019) for the trajectories of the vessel during SOP1. Two autonomous systems were installed in order to provide atmospheric and oceanic measurements, in the context of the HyMeX Long Observation Period (LOP). A GNSS antenna was installed at the front on the vessel Marfret Niolon for the duration of the HyMeX campaign. An example of the operational measurements which started on January 2012 are provided in Figure 2 with figures ranging from 2.2 m to 2.6 m. The data were post-processed in kinematic Precise Point Positioning with the software provided by Natural Resources Canada (Kouba and Héroux, 2001) and using high-resolution products provided by the International GNSS Service. The second source of independent data comes from wind data obtained from an airborne Doppler cloud-profiler radar named RASTA (Radar Airborne System Tool for Atmosphere (Bouniol et al., 2008; Protat et al., 2009; Delanoë et al., 2013)) that flew 45 days
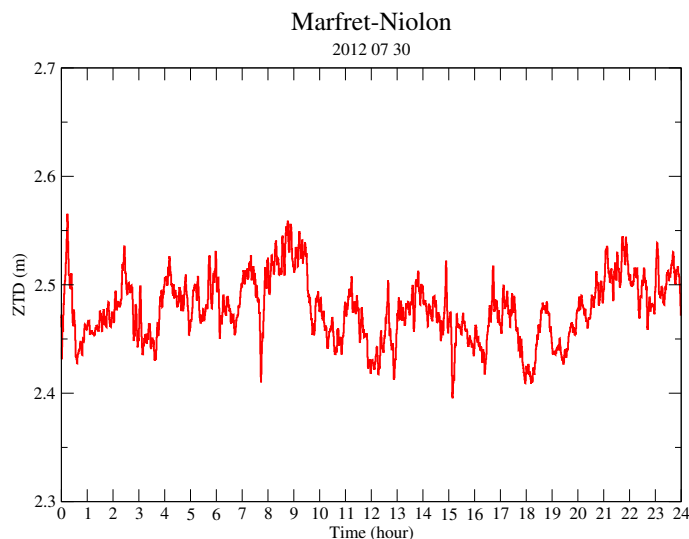
Figure 2. Evolution of the Zenithal total delay (ZTD, m) observed onboard the Marfret-Niolon ship during 25 October 2012.

during SOP1, on board the French Falcon 20 research aircraft. It allows the documentation of the microphysical properties and the horizontal components of the wind field in terms of vertical profiles.

140   In a second step, the forecast (range between +3 to +54 hours) quality is assessed in terms of surface parameters and precipitation scores. The surface parameters (temperature and relative humidity at 2 m and wind at 10 m) come from the HyMeX database which provides surface synoptic observations available over the AROME-WMED domain, together with additional hourly observations from Météo-France, AEMET and MeteoCat mesoscale networks. Some of these observations were assimilated to produce surface analyses. For the evaluation of the precipitation quality, the dense surface data set rain

145   gauge network available in the HyMeX data base (V4 version) has been used. Scores of 3 hourly accumulated precipitation from all analysis times on a given day are compared to the corresponding observed 24-h accumulated precipitation.

3   Impact of GNSS data on the analysis and first-guess quality

This section investigates the impact of assimilating the ground-based GNSS ZTD data on the numerical weather prediction model analysis and subsequent forecast quality. This data set represents the largest one in terms of total amount, even though it

150   represents a small fraction of assimilated data (1.85%). One of the key tool used to evaluate the performance of the assimilation system is to examine the First Guess departure (O-FG) and the Analysis departure (O-A) in terms of mean and root-mean square (RMS) values, O standing for Observation with the other assimilated observations.

Natural Hazards
and Earth System
Sciences
Discussions
Open Access
EGU

3.1 Impact on moisture field

Comparison to the Integrated Water Vapour (IWV) from the reprocessed GNSS observations (not independent from REANA as
155 the information from this data set is assimilated in this experiment) indicates that the best correlation, as expected, is obtained
for REANA (around 0.99), the second one being OPERGNSS (around 0.975) and the last one NOGNSS (around 0.96), as
shown in Figure 3. This result is confirmed when computing the RMS of the differences. A weak diurnal cycle of the scores
is noticed with a maximum correlation around 09 UTC and a minimum around 15 UTC. Concerning the standard deviation of
the differences, they are lower during the 3-9 UTC period and larger in the afternoon.
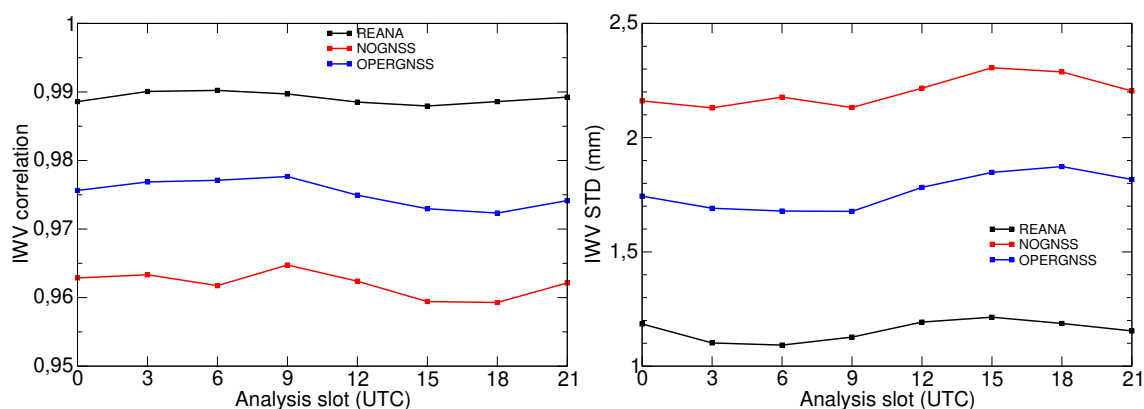
Figure 3. Correlation (upper panel) and standard deviations (lower panel, in mm) of integrated water vapour (IWV) content from reprocessed
GNSS observations (Bock et al., 2016) and AROME-WMED analyses (REANA in black NOGNSS in red and OPERGNSS in blue) as a
function of analysis slot (hours).

160 We then discuss the result of the statistics for the analysis and first-guess against radiosonde observations, which represents
a reference data set in data assimilation. First of all, as expected, the analysis RMS difference (solid lines) are smaller than
the FG difference (dashed lines) for the three simulations showing the expected behaviour of the minimisation during the
assimilation process (Figure 4). No impact can be seen on the analysis RMS differences, but a small positive impact is present
on the FG RMS difference, the lowest values being obtained with the REANA simulation, showing some positive impact of
165 the reprocessed GNSS ZTD on the independent data simulation at the 3-h forecast range. The largest improvement of the
assimilation of GNSS data is found between 600 and 850 hPa and the slight benefit of assimilating reprocessed GNSS data
appears between 700 and 850 hPa. The various analysis mean departures are very close to each others, with slight negative
values in the lower and mid troposphere (analysis too moist), as displayed in Figure 4 lower panel. Mean first-guess departures
are larger and homothetic, with stronger values for the REANA simulation, being the signature of a weak moist bias in the
170 corresponding analysis for the lower troposphere. The less biased first guess is the one from the NOGNSS experiment.

Radiances from SEVIRI (on board the geostationnary satellite Meteosat Second Generation (MSG)), sensitive to moisture
(channels WV 6.2 μm for upper-troposhere and 7.3 μm for mid-troposphere) are assimilated in AROME. They are an impor-
tant source of humidity information, especially over oceans where no information from GNSS nor radiosondes is available.

Basically no impact between the various experiments is found on the FG and AN statistics for these observations (figure not
175   shown).

The correlation between the various AROME-WMED ZTD analyses and corresponding independent (not assimilated) Mar-
fret Niolon observations is slightly and consistently higher for REANA than for NOGNSS and even for OPERGNSS (Figure
5). There is a correlation maximum around 09 UTC, and a minimum around 15 UTC. The mean ZTD is quite similar in all
experiments, with a maximum at 09 UTC and a minimum around 00 UTC. A moist bias is found in all simulations when
180   compared to the mean observation in grey shown in Figure 5. The magnitude of this relative positive (moist) bias is around 0.5
percent. Although the sample size of Marfret-Niolon data set is rather small (around 1000 collocations), this is a original result
and makes clear that the REANA experiment produces the best reanalysis, and the best 3-hour forecasts.
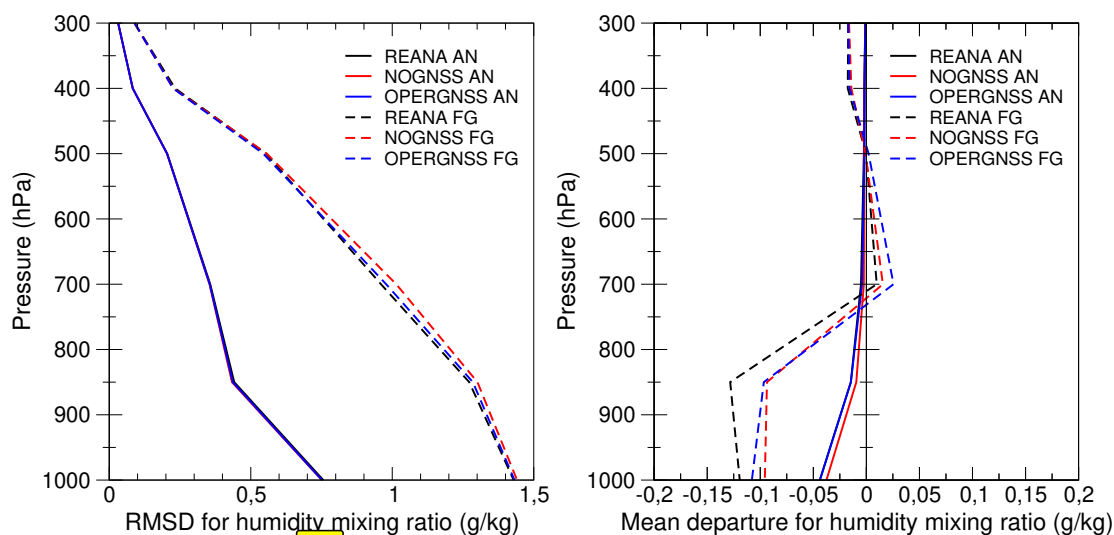
Figure 4. Root mean square differences (top panel) and mean (lower panel) for Analysis (AN solid lines) and First-Guess (FG, dashed lines)
departures against assimilated radio-sounding observations for (mixing ratio, g/kg; REANA in black, NOGNSS in red and OPERGNSS in
blue.)

3.2   Impact on wind field

Analysis and First-guess quality has been evaluated against RASTA (Radar Airborne System Tool for Atmosphere) Doppler
185   winds (Borderies et al., 2019). This airborne radar was on board Falcon 20 aircraft and provided 33083 wind observations
over the Mediterranean area as illustrated in Figure 7, where only few wind data from conventional observations are available.
Worth to remind that the data from this instrument were not assimilated in REANA. This data set thus represents an additional
independent information for the evaluation of our denial experiments.

Table 3 provides the root mean square errors for wind calculated with these data. The RMSE for background and analysis are
190   lower in REANA than in the other two experiments. The analysis RMSE for OPERGNSS is lower than the one for NOGNSS.
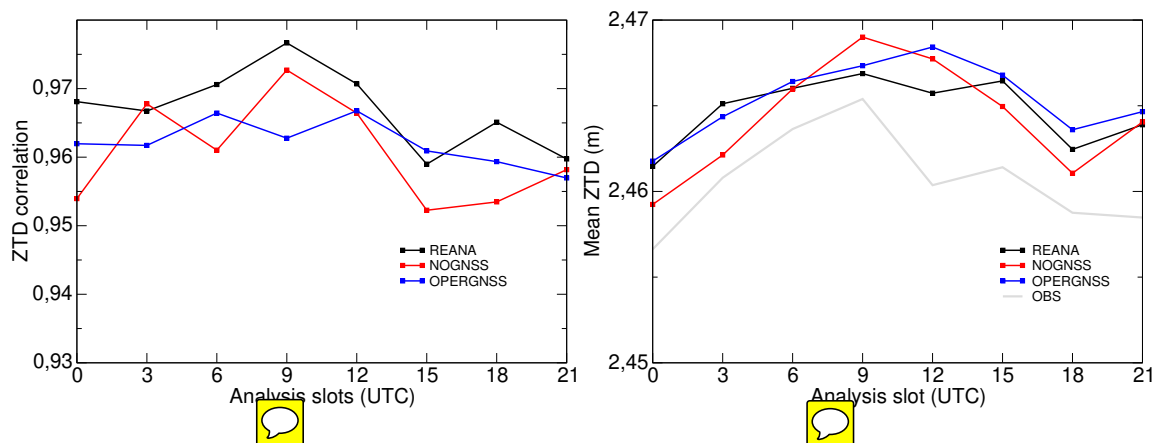
Figure 5. Correlation of the differences between zenithal total delays (ZTD) between REANA (Black), NOGNSS (red), OPERGNSS (blue) analyses and corresponding Marfret-Niolon observations as a function of analysis time in the upper panel; mean value in the lower panel, the grey line corresponding to observations.
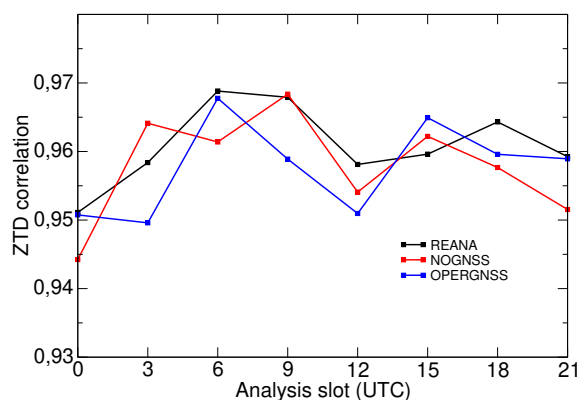

Figure 6. Correlation between zenithal total delay forecasted by AROME-WMED at the 3-hour forecast range and observations from Marfret Niolon.

Experiment	AN RMSE	FG RMSE
REANA	5.59	5.87
NOGNSS	5.63	5.97
OPERGNSS	5.60	5.92

Table 3. Analysis (AN) and First Guess (FG) Root Mean Square Errors (RMSE) computed with respect to RASTA observations (sample size 33083 observations) for REANA, NOGNSS and OPER GNSS experiments.
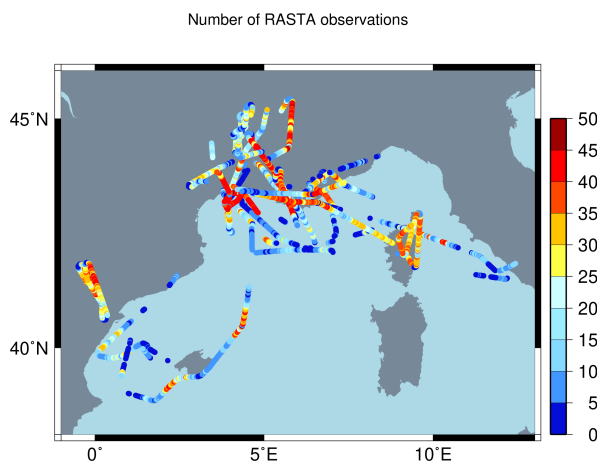
Figure 7. Location of RASTA observations during the HyMeX Special Observation Period 1. Coloured dots represent the number of wind data available per profile.

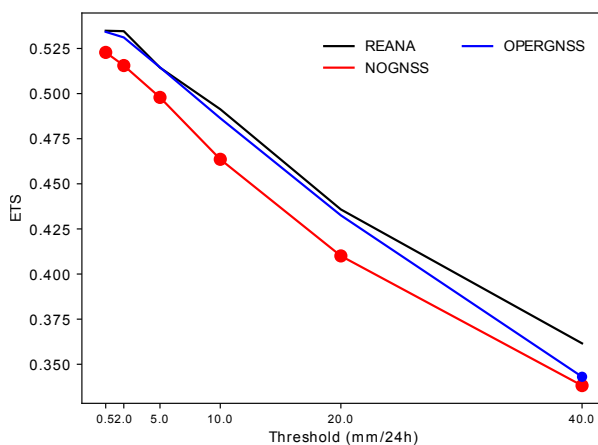## 3.3 Impact on short-range precipitation

Figure 8. Equitable Threat Score (ETS) for the 24-h accumulated precipitation from the sum of the eight 3-h forecasts used as background of the data assimilation cycle each day of the period from 5 September to 5 November 2012. Results for REANA are displayed in black, for NOGNSS in red and GNSS OPER in blue. Dots indicate that the difference between the curves and the REANA curve as a reference is statistically significant at a 0.95 confidence threshold using a bootstrap test.

Figure 8 shows that the Equitable Threat Score (ETS) of the 24-h accumulated precipitation computed with the sum of the 3-h precipitation from the 8 analysis times is improved with the assimilation of GNSS ZTD data compared to the NOGNSS experiment. It represents an evaluation of the background quality. The difference is statistically significant for each threshold.

195 When comparing the assimilation of reprocessed data to the real-time ones, the ETS for precipitation is slightly better with

the reprocessed data set but the differences are not significant except for the 40 mm/day threshold. However this threshold represents only few cases. Overall, the background quality is improved with the assimilation of GNSS observations and the data reprocessing brings improvement in terms of precipitation from 3-hour forecast even though this benefit is not significant.

4 Impact of GNSS data on medium term forecast

200   The impact of the GNSS data has also been assessed for longer forecast range (3 to 54-h). The effect of the assimilation of the GNSS data on the correlation with IWC from the GNSS data set is maximal for the analysis and decreases up to the 30-h forecast range (Figure 9) as the general impact of the initial conditions on the forecast performances reduces. A similar behaviour is found with the standard deviations of the differences between observed IWC and simulated one from the three experiments.
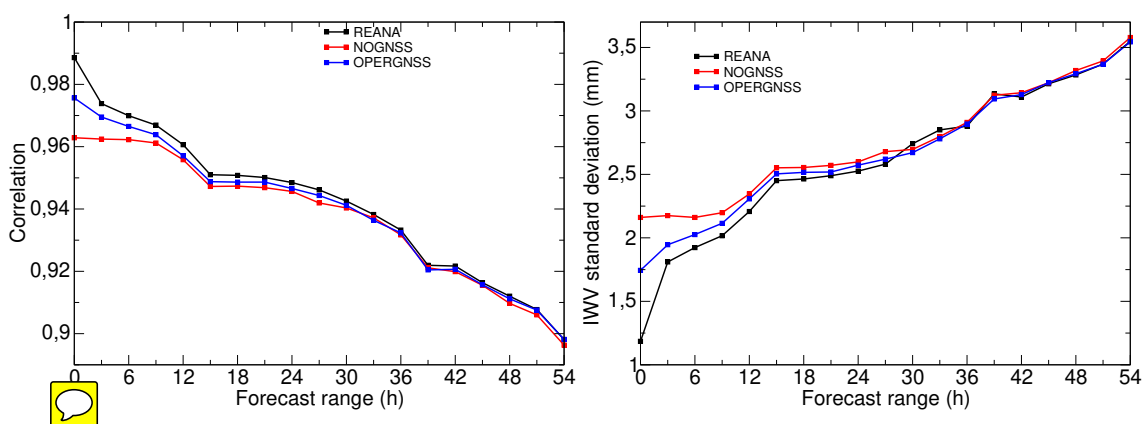

Figure 9. Correlation (top panel) and standard deviations (bottom panel) (mm) of integrated water vapour content between AROME-WMED forecasts and reprocessed GNSS observations (Bock et al., 2016) as a function of forecast range (hours).

205   Compared to the observed ZTD from the Marfret Niolon ship, the signal is more noisy because of a smaller dataset but in overall the correlation for the NOGNSS is lower and the standard deviations are in general higher for the NOGNSS forecasts (Figure 10).

The forecast quality has also been evaluated against surface data. No impact was found on temperature at 2 meters or on 10 m wind. A small impact was found on relative humidity at 2 meters (Figure 11). A reduction of the bias is noticed with REANA

210   during the first 9-h of the forecast compared to OPER GNSS and NOGNSS. From 12-h onwards the results for REANA and OPERGNSS are similar. Regarding the standard deviation, it is smaller for REANA between 0 and 9-h than for NOGNSS and GNSS OPER and between 21 and 27-h forecast range than for NOGNSS. This difference represents more than 2 % of improvement. For the other forecast ranges the differences are lower than 1%.

The impact of the assimilation of GNSS data on the 24-h accumulated precipitation from the forecast initialized at 06 UTC

215   is less clear. The improvement of the GNSS data reprocessing compared to the real time data set is beneficial for all thresholds
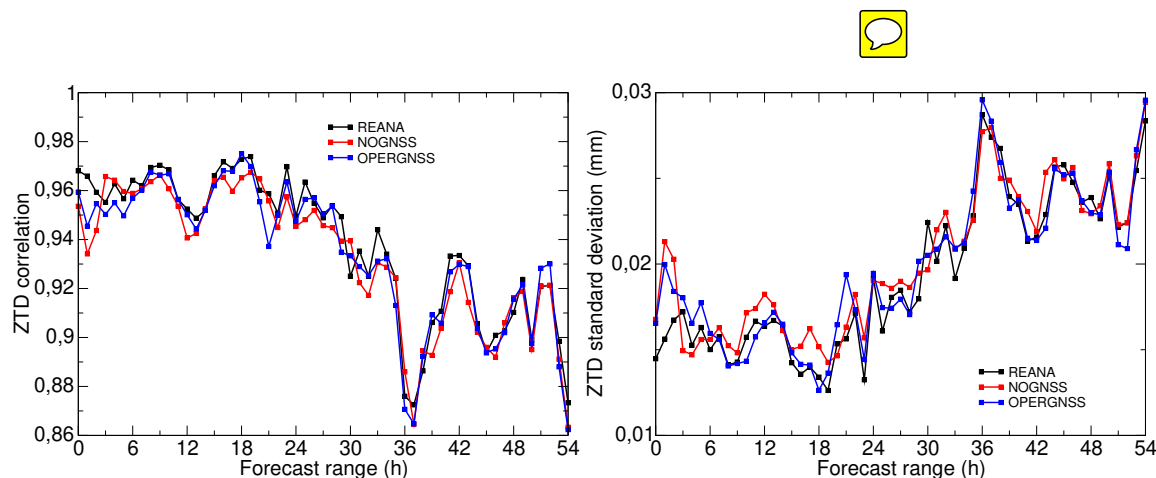
Figure 10. Correlation and standard deviations of zenithal total delays forecasted with AROME-WMED experiments with respect to Marfret Niolon data.
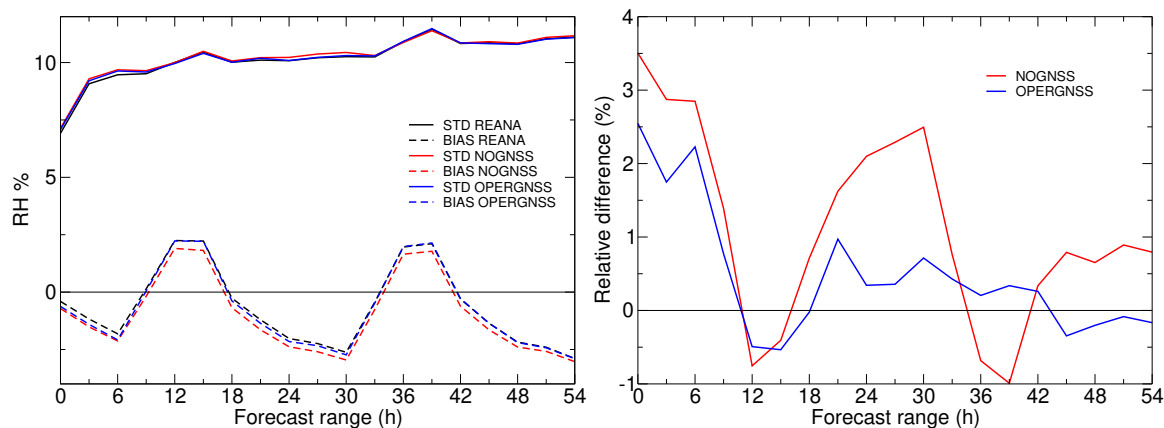

Figure 11. Bias (forecast minus observations, dashed lines) and standard deviations (solid lines) computed with relative humidity at 2 meters (top panel) and relative root mean square differences (% bottom panel) with respect to REANA.

except for the 2mm/day (where the ETS is better for OPERGNSS) and is statistically significant for large thresholds (10 and 20 mm/day, Figure 12). The difference between REANA ETS and NOGNSS ETS values is not significant. When examining scores for precipitation forecasts between 30-h and 54-h, there is a small significant degradation of the ETS for the 2 mm/day with the NOGNSS experiment and a small improvement with the OPERGNSS for the 40 mm/day (Figure 13).

5 Other impact studies

As previously mentioned we performed other impact studies with wind profilers, lidar data and Spanish radar data.
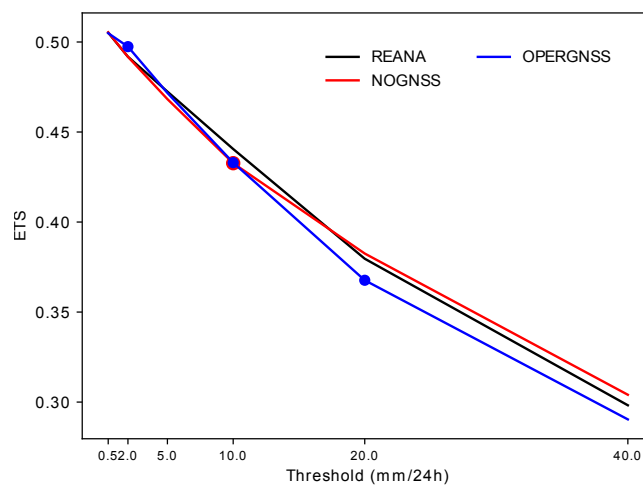
13

Figure 12. Equitable Threat Score of the 24-h accumulated precipitation from the 6-30 hour forecast range of the long forecast initialized at 00 UTC each day of the period from 5 September to 5 November 2012 computed over the AROME-WMED domain with rain gauges of the HyMeX database (version 4). Dots indicate that the difference between the curves is statistically significant.
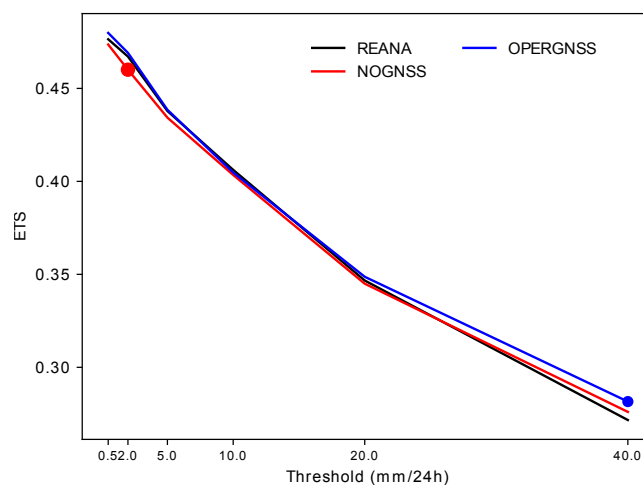

Figure 13. Equitable Threat Score of 24 h accumulated precipitation from the 30 to 54 hour forecast range of the long forecast initialized at 00 UTC each day of the period from 5 September to 5 November 2012 computed over the AROME-WMED domain with rain gauges of the HyMeX database (version 4). Dots indicate that the difference between the curves is statistically significant.

14

5.1 Wind profilers

No impact of the assimilation of wind profiler data is found except on wind fiel. Small impact is noticed in terms of wind RMS differences of background and analysis departures for radiosondes, aircraft and satellite winds (Figure 14). The largest

225 impact is a decrease of -0.08 m/s for the radiosonde FG RMS differences at 300 hPa. Concerning the AN RMS differences, the improvement (SATOB) or degradation (AIREP and TEMP) are very small. The largest value obtained at 200 hPa are due to the small number of data available for the computation.
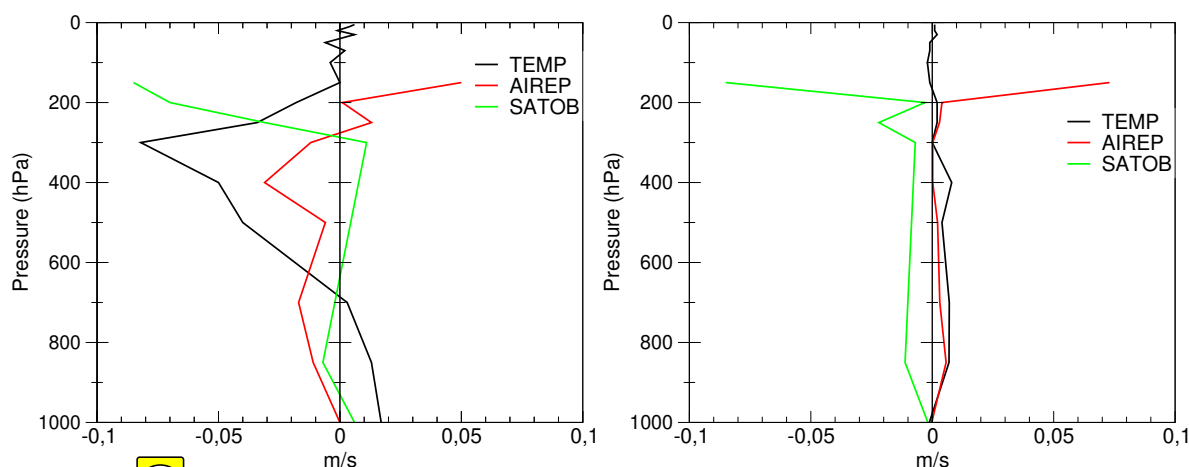

Figure 14. First-Guess (upper-plot) and analysis (lower plot) RMS differences (REANA-NOWPROF experiments) computed against TEMP (black), AIREP (red) and SATOB (green) observations for the zonal wind component (m/s); negative value correspond to a positive impact of wind profiler.

A small improvement but not significant (Figure 15), appears on the ETS of the 24 h accumulated precipitation accumulated from the 6 to 30 hour forecast ranges.

5.2 Ground-based and airborne lidar data

As discussed in Section 2.2, humidity profiles retrieved from ground-based and air-borne lidars have been assimilated in the REANA experiment. In Figure 1, the trajectories of all ATR-42 flights are plotted, together with the localization of the two ground-based lidars. The denial NOLIDAR experiment results are close to the reanalysis ones as these data represent very few additional data and are located over ocean where few observations are available for the comparison. No impact of the Lidar

235 data is found when comparing the various analyzed ZTD to the Marfret-Niolon corresponding observations. These results agree with the Bielli et al. (2012) study where no significant impact where found on the 24-h accumualted precipitation.
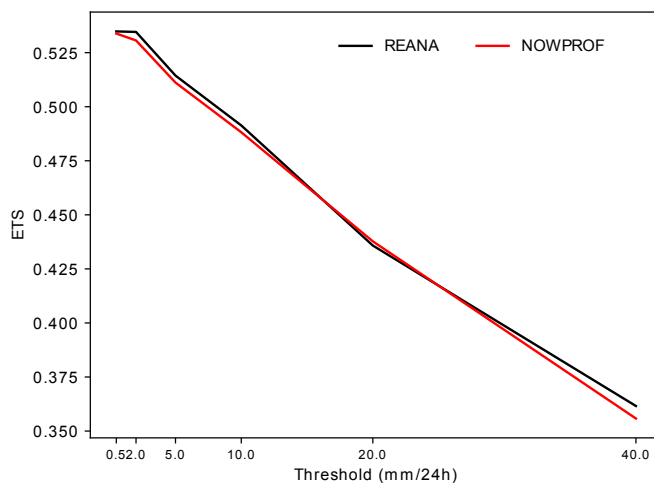
Figure 15. Equitable Threat Score of 24 h accumulated precipitation from the 6 to 30 hour forecast ranges of the long forecast starting at 00 UTC each day of the period from 5 September to 5 November 2012 computed over the AROME-WMED domain with rain gauges of the HyMeX database (version 4). The lack of dots indicates that the difference between the curves is not significant. REANA is plotted in black and NOWPROF in red.

5.3 Spanish radars

No significant impact has been noticed over the HyMeX domain however, when focusing on the scores over the Iberic Peninsula, we obtained a positive and significant impact of the assimilation of Spanish radar data on the ETS for the 24-h accumulated precipitation from the sum of the 8 3-h precipitation background forecast (Figure 16). This impact also remains in longer forecast ranges as the ETS for the 24-h precipitation accumulation between 6-h and 30-h forecast ranges is improved with the assimilation of Spanish radars for thresholds between 0.5 and 20 mm/24h (Figure 17). This impact does not remains at longer forecast ranges (Figure 18). These results are in good agreement with Wattrelot et al. (2014) study which found an improvement of the short term precipitation forecast scores. However contrary to the aforementioned study, we obtained a significant improved of the 24-h precipitation accumulation between 6-h and 30-h forecast ranges over the Iberic Peninsula.

6 IOP16 case study

During HyMeX SOP1, IOP16a was dedicated to HPE that occured over Cévennes-Vivarais (CV) in France and later on, in Italy (IOP16b) on 25-26 October; this event was associated with locally flash-flooding and several casualties. This off-shore convection case is well documented in Duffourg et al. (2016). On the 26th - 00 UTC active convection was occuring over Catalunia; this area of intense convective activity crossed the Gulf of Lion reaching the French Mediterranean coast around 06 UTC and later on, in the evening the Italian Ligurian coast. It is well known that the associated convective systems are usually fed with moisture, during their early stage over the warm Mediterranean sea. A moist conditionally unstable south-
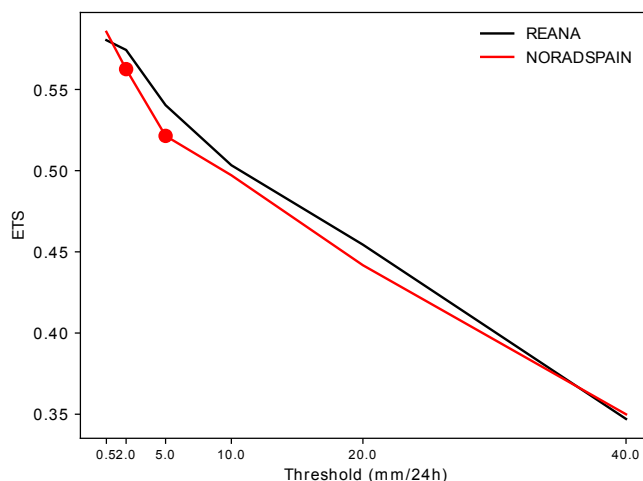
Figure 16. Equitable Threat Score (ETS) for the 24-h accumulated precipitation obtained from the sum of eight 3-h forecasts used as background of the data assimilation cycle each day of the period from 5 September to 5 November 2012 computed over the AROME-WMED domain with rain gauges of the HyMeX database (version 4). Results for REANA are displayed in black, for NORADSPAIN in red. Dots indicate that the difference between the curves is statistically significant.
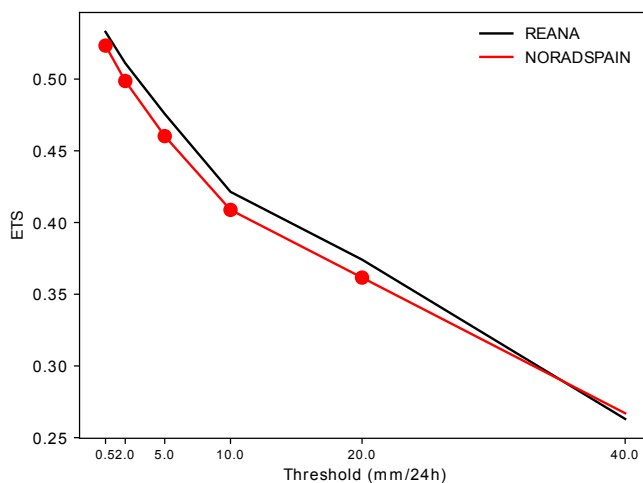

Figure 17. Equitable Threat Score (ETS) for the 24-h accumulated precipitation from the 6 to 30 hour forecast ranges initialized at 00 UTC each day of the period from 5 September to 5 November 2012 computed over the AROME-WMED domain with rain gauges of the HyMeX database (version 4). Results for REANA are displayed in black, for NORADSPAIN in red. Dots indicate that the difference between the curves is statistically significant.

Figure 18. Equitable Threat Score (ETS) for the 24-h accumulated precipitation from the 30 to 54 hour forecast ranges initialized at 00 UTC each day of the period from 5 September to 5 November 2012 computed over the AROME-WMED domain with rain gauges of the HyMeX database (version 4). Results for REANA are displayed in black, for NORADSPAIN in red. Dots indicate that the difference between the curves is statistically significant.
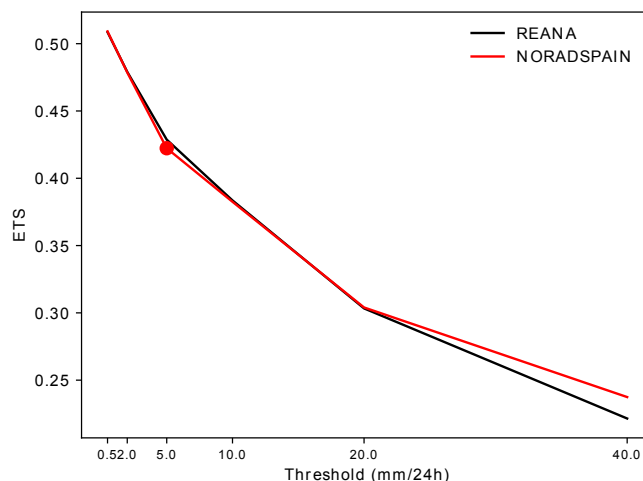
western flux is therefore found in the lower troposphere (Figure 19) with a low-level jet by the Candillargues radar around 09-12 UTC, associated to a slow evolving weak pressure low (around 995 hPa) localized over southern France on the 26th

255   mid-day. Moreover, low level convergence is reinforced by the complex orography (Cévennes ridge of the Massif-Central and Alps in France) triggering convection. An upper south-westerly wind jet is observed above 500 hPa (Figure 19); in the evening of the 25th the wind rotates to the west on the CV area as shown by the Candillargues UHF radar.

During 25th and 26th October period, many deep convective systems developed over the Northwestern Mediterranean. Although accumulated surface precipitation from Friday 26th at 18 UTC to Saturday Oct. 27th at 06 UTC over southern

260   France only reached around 150 mm in 24h, very strong hourly rates (near 50 mm/1h) were recorded, with intense river discharges (Ardèche, Gardons and Gapeau rivers for example). Such intense rainfall amounts led to local flash-floods and 2 casualties in the Var region. In fact as shown in Figure 20, three local precipitation maxima appear on the observed 24-hour accumulated rainfall amount (25th October - 06 UTC to 26th October - 06 UTC) on the Mediteranean costal area of France and Italy (Liguria Tuscany region); a first elongated one in the Cévennes area (more than 150 mm, M1) and a small second one

265   close to the coast (around 100 mm, M2).

Figure 21 shows the 24-h accumulated precipitation between the 6-h and 30-h forecasts for the different experiments considered in this study. The REANA 24-hour accumulated rainfall (+30 - +06 hours forecast range) simulation agrees to the observations for both M1 and M2 systems. The NOLIDAR experiment is very close to REANA, this is consistent with the fact that the amount of additional lidar data is fairly small in REANA when compared to NOLIDAR. The strongest impact is found

270   when no GNSS data are assimilated (NOGNSS run): M1 and M2 are strongly underestimated; surprisingly the OPERGNSS experiment leads to an accurate forecast of M2, but underestimates the southwestward extension of M1. Finally a strong neg-
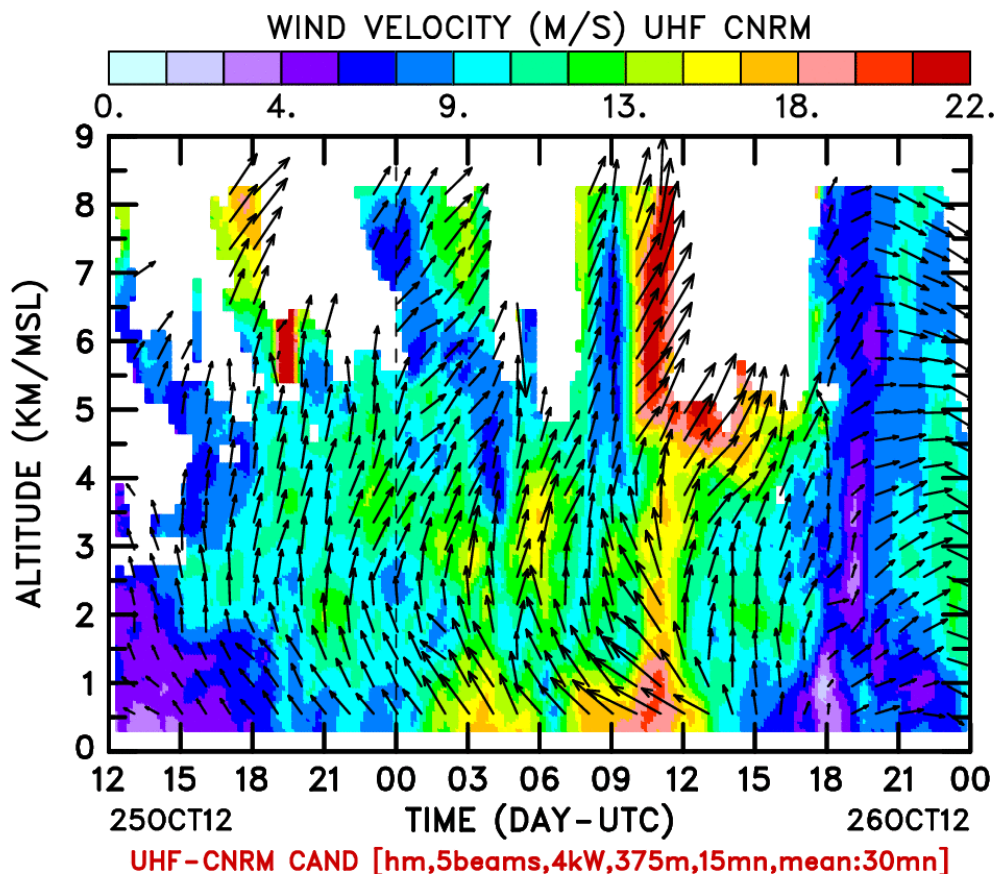
Figure 19. Time-height cross-section of the wind measured by the Candillargues UHF radar for IOP16. Horizontal wind components are represented by the black arrows (meteorological convention), and wind speed in colour.

ative impact is found with the NOWPROF simulation which misses M2 and does not reproduce correctly M1. Over Italy, the gain brought by the observations is not so evident but it is quite well known in data impact studies that the assimilation of observation does not always improve the forecast at each analysis time but in overall.

275   **7   Conclusions**

The AROME-WMED model was originally developed to study and forecast heavy-precipitating Mediterranean events during the Special Observation Periods (SOPs) of the HyMeX programme. Two reanalyses were undertaken after the HyMeX autumn campaign for the first SOP. A first one was carried out just after the campaign to provide the same model configuration over the whole SOP1 period because a version upgrade of AROME-WMED occurred during the period. A second reanalysis, performed
280   a few years after, accounted for as many data as possible from the experimental campaign (i.e., lidar and dropsonde humidity
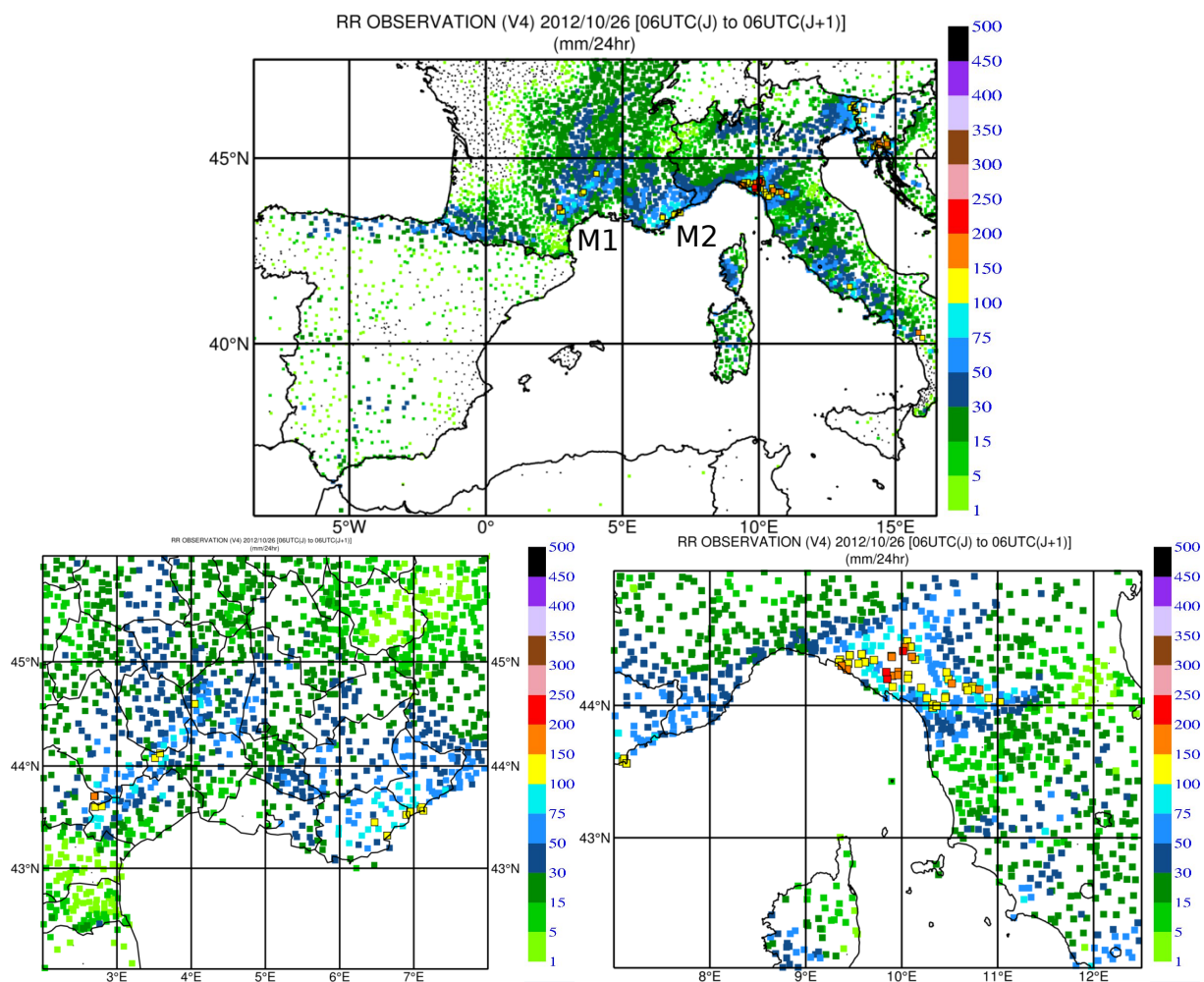
Figure 20. 24 h accumulated precipitation (mm) between 26 October 06 UTC and 27 October 2012 at 06 UTC over the AROME-WMED domain (upper plot) and zoom over the Cevennes region (left lower plot) and over North of Italy (right lower plot).
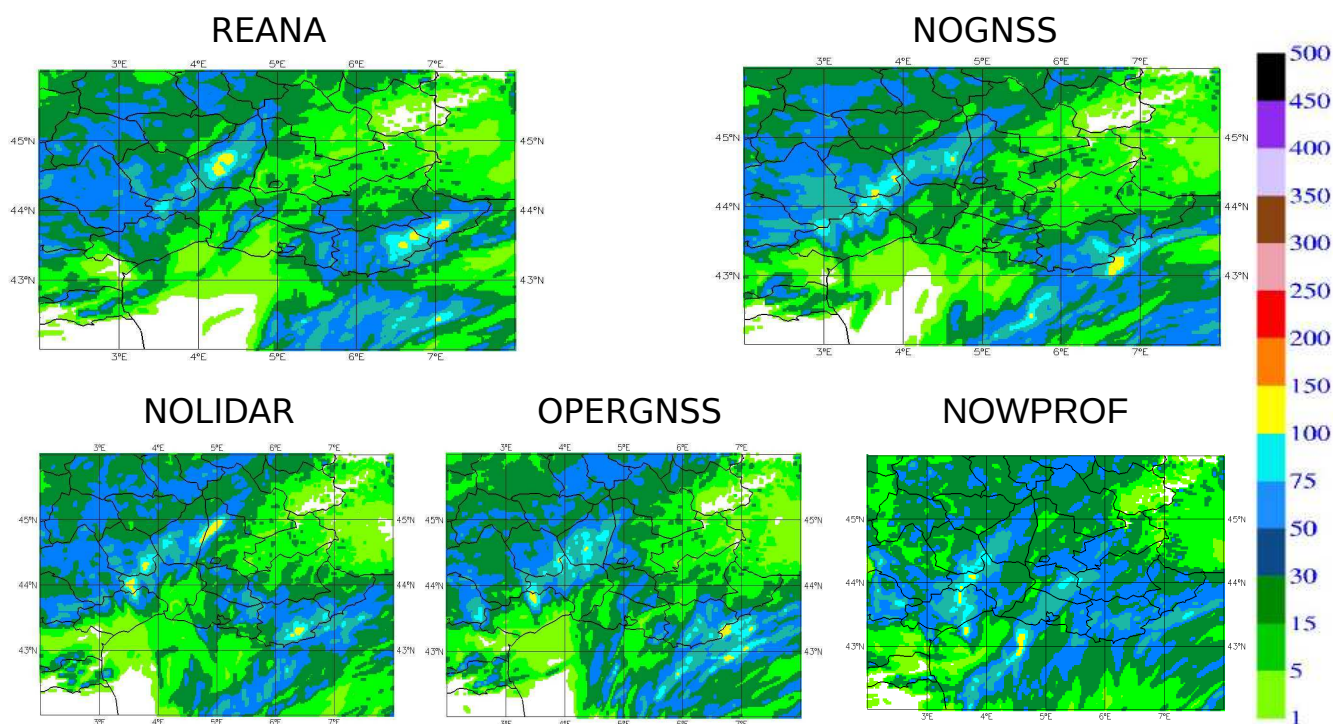
Figure 21. Same as Figure 20 but for 24h accumulated precipitation forecasted by (a) REANA, (b) NOGNSS, (c) NOLIDAR (d) OPERGNSS and (e) NOWPROF experiments, for the +30 - +06 forecast range.

profiles) or from reprocessed data sets (such as GNSS ground station ZTD, wind profilers, high-vertical resolution radiosondes, and Spanish Doppler radars). It also benefited from a updated version of the AROME code.

Previous studies such as Duffourg and Ducrocq (2011) Ricard et al. (2012) or Bresson et al. (2012), have shown the interest of an accurate description of the low-level moist flow feeding mesoscale convective systems. In this study the impact of various
285 data set related to humidity and wind on the forecast quality from this comprehensive reanalysis is investigated over the 2-month period. Many data sets of the Special Observation Period 1 of the HyMeX campaign have been considered here. The reprocessed GNSS data set (Bock et al. (2016)) were removed and replaced with the operational data set used in the real-time AROME-WMED version. We examined the humidity data provided by ground based and airborne lidars. The impact of the reprocessed wind profilers and the Spanish radar data was also evaluated. The impact of these data sets was assessed through
290 Observing system Experiments which consist of removing the data sets and to compare forecast quality from these denial experiments to a reference which includes all data sets. The selected data sets were research observations (water vapour lidars) or reprocessed data (from ground based GNSS receivers or wind profilers). They represented a modest part of the assimilated data amounts and their impact was thus expected to be small.

21

295 Our study finds a small positive impact on humidity forecast at short term ranges of the reprocessed GNSS ground based zenithal total delay assimilation. This data set is evenly distributed over the AROME-WMED domain and provided at each analysis time information on integrated water vapour. The impact of the data reprocessing was also studied and even if a positive impact is observed, this improvement is not statistically significant compared to the impact of the real-time data. Given the impact of ground-based GNSS, there is also an interest in continuing work to assimilate GNSS data over ocean surfaces.

300 Small impacts on wind fields were also observed for wind profilers. No impact from Lidar data was found except when comparing with RASTA data located over the Mediterranean Sea. Since this data set represents a very small fraction of assimilated data, this may explain the absence of impact. In addition they were not assimilated at their full available temporal frequency but just once every 3 hours.

Spanish radar data assimilation improves the short term quality of the background as noticed on the 24-h accumulated precipitation of the eight 3-h background forecasts for each day but only over the Iberic Peninsula with no clear impact over
305 the HyMeX domain. It is interesting to stress that this impact remains during the first 30-h of the forecast but without any remote impact over the rest of the AROME-WMED domain. More impact could possibly be obtained if the data were provided with additional scan elevations.

Our study shows that it is required to have well spatially distributed and frequent data sets to get an overall impact from it in terms of analysis and forecast skills. Other data sets may have an impact but it remains local. With newer data assimilation
310 systems, making use of observations at higher temporal frequency as it is the case with the current AROME-France model (Brousseau et al., 2016), it is likely that surface observations or the remote sensing data such as radars, GNSS or SEVIRI available for each hourly analysis in this study would have a greater impact on analyses and forecasts. Moreover new data assimilation systems such as the 4D-Var or the 4D-Envar are under development for convective scale models (Gustafsson et al., 2018) and will allow to account for very frequent data . Therefore, they are expected to enhance the impact of observations
315 such as the ground-based GNSS or SEVIRI radiances available several times an hour. In the future, the impact of the Infra-Red Sounder onboard Meteosat Third Generation will benefit from these new data assimilation systems as this sounder will provide observations every 30 minutes over the AROME domain and especially over the oceans.

Code availability. The source code of AROME-WMED, derived from the operational AROME code cannot be obtained.

Data availability. The analyses and the forecast fields are available in the HyMeX database (http://mistrals.sedoo.fr/HyMeX/, last ac-
320 cess 19 August 2019). The final (second) reanalysis labelled REANA in this paper is available at https://doi.org/10.14768/MISTRALS-HYMEX.1492 (Fourrié and Nuret, 2017).

Natural Hazards
and Earth System
Sciences
Discussions

Author contributions. NF and MN prepared and carried out all the numerical experiments of the reanalysis and the OSEs. They investigated the results, and wrote the paper with the help of all the coauthors. PBr and OC helped to investigate the results by performing diagnostics and verification computations.

325 *Competing interests.* The authors declare that they have no conflict of interest.

References

Benjamin, S. G., Schwartz, B. E., Szoke, E. J., and Koch, S. E.: The Value of Wind Profiler Data in U.S. Weather Forecasting, Bulletin of the American Meteorological Society, 85, 1871–1886, https://doi.org/10.1175/BAMS-85-12-1871, https://doi.org/10.1175/BAMS-85-12-1871, 2004.

335 Bielli, S., Grzeschik, M., Richard, E., Flamant, C., Champollion, C., Kiemle, C., Dorninger, M., and Brousseau, P.: Assimilation of water-vapour airborne lidar observations: impact study on the COPS precipitation forecasts, Quarterly Journal of the Royal Meteorological Society, 138, 1652–1667, https://doi.org/10.1002/qj.1864, 2012.

Bock, O., Bosser, P., Pacione, R., Nuret, M., Fourrié, N., and Parracho, A.: A high-quality reprocessed ground-based GPS dataset for atmospheric process studies, radiosonde and model evalu ation, and reanalysis of HyMeX Special Observing Period, Quart. J. Roy.

340 Meteorol. Soc., 142, 56–71, https://doi.org/10.1002/qj.2701, https://rmets.onlinelibrary.wiley.com/doi/abs/10.1002/qj.2701, 2016.

Boniface, K., Ducrocq, V., Jaubert, G., Yan, X., Brousseau, P., Masson, F., Champollion, C., Chéry, J., and Doerflinger, E.: Impact of high-resolution data assimilation of GPS zenith delay on Mediterranean heavy rainfall forecasting, Annales Geophysicae, 27, 2739–2753, https://doi.org/10.5194/angeo-27-2739-2009, https://www.ann-geophys.net/27/2739/2009/, 2009.

Borderies, M., Caumont, O., Delanoë, J., Ducrocq, V., and Fourrié, N.: Assimilation of wind data from airborne Doppler cloud-profiling radar

345 in a kilometre-scale NWP system, Natural Hazards and Earth System Sciences, 19, 821–835, https://doi.org/10.5194/nhess-19-821-2019, https://www.nat-hazards-earth-syst-sci.net/19/821/2019/, 2019.

Bouniol, D., Protat, A., Plana-Fattori, A., Giraud, M., Vinson, J.-P., and Grand, N.: Comparison of Airborne and Spaceborne 95-GHz Radar Reflectivities and Evaluation of Multiple Scattering Effects in Spaceborne Measurements, Journal of Atmospheric and Oceanic Technology, 25, 1983–1995, https://doi.org/10.1175/2008JTECHA1011.1, https://doi.org/10.1175/2008JTECHA1011.1, 2008.

350 Bresson, E., Ducrocq, V., Nuissier, O., Ricard, D., and de Saint-Aubin, C.: Idealized numerical simulations of quasi-stationary convective systems over the Northwestern Mediterranean complex terrain, Q.J.R. Meteorol. Soc., 138, 1751–1763, 2012.

Brousseau, P., Berre, L., Bouttier, F., and Desroziers, G.: Background error covariances for a convective-scale data-assimilation system : AROME-France 3D-Var, Quarterly Journal of the Royal Meteorological Society, 137, 409–422, https://doi.org/10.1002/qj.750, 2011.

Brousseau, P., Seity, Y., Ricard, D., and Léger, J.: Improvement of the forecast of convective activity from the AROME-France system,

355 Quarterly Journal of the Royal Meteorological Society, 142, 2231–2243, https://doi.org/10.1002/qj.2822, 2016.

Caniaux, G., Redelsperger, J.-L., and Lafore, J.-P.: A numerical study of the stratiform region of a fast-moving squall line. Part I: General description and water and heat budgets, Journal of the Atmospheric Sciences, 51(14), 2046–2074, 1994.

Chazette, P., Flamant, C., Shang, X., Totems, J., Raut, J.-C., Doerenbecher, A., Ducrocq, V., Fourrié, N., Bock, O., and Cloché, S.: A multi-instrument and multi-model assessment of atmospheric moisture variability over the western Mediterranean during HyMeX, Quarterly

360 Journal of the Royal Meteorological Society, 142, 7–22, https://doi.org/10.1002/qj.2671, https://rmets.onlinelibrary.wiley.com/doi/abs/10.1002/qj.2671, 2016.

Courtier, P., Freydier, C., Rabier, F., and Rochas, M.: The ARPEGE Project at Météo-France, ECMWF Seminar Proceedings, 7, 193–231, 1991.

Delanoë, J., Protat, A., Jourdan, O., Pelon, J., Papazzoni, M., Dupuy, R., Gayet, J.-F., and Jouan, C.: Comparison of Airborne In Situ,

365 Airborne Radar–Lidar, and Spaceborne Radar–Lidar Retrievals of Polar Ice Cloud Properties Sampled during the POLARCAT Campaign, Journal of Atmospheric and Oceanic Technology, 30, 57–73, https://doi.org/10.1175/JTECH-D-11-00200.1, https://doi.org/10.1175/JTECH-D-11-00200.1, 2013.

Di Girolamo, P., Flamant, C., Cacciani, M., Richard, E., Ducrocq, V., Summa, D., Stelitano, D., Fourrié, N., and Saïd, F.: Observation of low-level wind reversals in the Gulf of Lion area and their impact on the water vapour variability, Quarterly Journal of the Royal Meteorological Society, 142, 153–172, https://doi.org/10.1002/qj.2767, https://rmets.onlinelibrary.wiley.com/doi/abs/10.1002/qj.2767, 2016.

Drobinski, P., Ducrocq, V., Alpert, P., Anagnostou, E., Béranger, K., Borga, M., Braud, I., Chanzy, A., Davolio, S., Delrieu, G., Estournel, C., Boubrahmi, N. F., Font, J., Grubišić, V., Gualdi, S., Homar, V., Ivančan-Picek, B., Kottmeier, C., Kotroni, V., Lagouvardos, K., Lionello, P., Llasat, M. C., Ludwig, W., Lutoff, C., Mariotti, A., Richard, E., Romero, R., Rotunno, R., Roussot, O., Ruin, I., Somot, S., Taupier-Letage, I., Tintore, J., Uijlenhoet, R., and Wernli, H.: HyMeX: A 10-Year Multidisciplinary Program on the Mediterranean Water Cycle, Bulletin of the American Meteorological Society, 95, 1063–1082, https://doi.org/10.1175/BAMS-D-12-00242.1, https://doi.org/10.1175/BAMS-D-12-00242.1, 2014.

Ducrocq, V., Braud, I., Davolio, S., Ferretti, R., Flamant, C., Jansa, A., Kalthoff, N., Richard, E., Taupier-Letage, I., Ayral, P.-A., Belamari, S., Berne, A., Borga, M., Boudevillain, B., Bock, O., Boichard, J.-L., Bouin, M.-N., Bousquet, O., Bouvier, C., Chiggiato, J., Cimini, D., Corsmeier, U., Coppola, L., Cocquerez, P., Defer, E., Delanoë, J., Girolamo, P. D., Doerenbecher, A., Drobinski, P., Dufournet, Y., Fourrié, N., Gourley, J. J., Labatut, L., Lambert, D., Coz, J. L., Marzano, F. S., Molinié, G., Montani, A., Nord, G., Nuret, M., Ramage, K., Rison, W., Roussot, O., Said, F., Schwarzenboeck, A., Testor, P., Baelen, J. V., Vincendon, B., Aran, M., and Tamayo, J.: HyMeX-SOP1: The Field Campaign Dedicated to Heavy Precipitation and Flash Flooding in the Northwestern Mediterranean, Bulletin of the American Meteorological Society, 95, 1083–1100, https://doi.org/10.1175/BAMS-D-12-00244.1, https://doi.org/10.1175/BAMS-D-12-00244.1, 2014.

Duffourg, F. and Ducrocq, V.: Origin of the moisture feeding the Heavy Precipitating Systems over Southeastern France, Nat. Hazards Earth Syst. Sci., 11, 1163–1178, 2011.

Duffourg, F., Nuissier, O., Ducrocq, V., Flamant, C., Chazette, P., Delanoë, J., Doerenbecher, A., Fourrié, N., Di Girolamo, P., Lac, C., Legain, D., Martinet, M., Saïd, F., and Bock, O.: Offshore deep convection initiation and maintenance during HyMeX IOP16a heavy precipitation event, Quaterly Journal of the Royal Meteorological Society, 142, 259–274, 2016.

Fourrié, N., Bresson, E., Nuret, M. andJany, C., Brousseau, P., Doerenbecher, A., Kreitz, M., Nuissier, O., Sevault, E., Bénichou, H., Amodei, M., and Pouponneau, F.: AROME-WMED, a real-time mesoscale model designed for the HyMeX special observation periods, Geoscientific Model Development, 8, 1919–1941, https://doi.org/10.5194/gmd-8-1919-2015, https://www.geosci-model-dev.net/8/1919/2015/, 2015.

Fourrié, N., Nuret, M., Brousseau, P., Caumont, O., Doerenbecher, A., Wattrelot, E., Moll, P., Bénichou, H., Puech, D., Bock, O., Bosser, P., Chazette, P., Flamant, C., Di Girolamo, P., Richard, E., and Saïd, F.: The AROME-WMED reanalyses of the first special observation period of the Hydrological cycle in the Mediterranean experiment (HyMeX), Geoscientific Model Development, 12, 2657–2678, https://doi.org/10.5194/gmd-12-2657-2019, https://www.geosci-model-dev.net/12/2657/2019/, 2019.

Grzeschik, M., Bauer, H.-S., Wulfmeyer, V., Engelbart, D., Wandinger, U., Mattis, I., Althausen, D., Engelmann, R., Tesche, M., and Riede, A.: Four-Dimensional Variational Data Analysis of Water Vapor Raman Lidar Data and Their Impact on Mesoscale Forecasts, Journal of Atmospheric and Oceanic Technology, 25, 1437–1453, https://doi.org/10.1175/2007JTECHA974.1, 2008.

Gustafsson, N., Janjić, T., Schraff, C., Leuenberger, D., Weissmann, M., Reich, H., Brousseau, P., Montmerle, T., Wattrelot, E., Bučánek, A., Mile, M., Hamdi, R., Lindskog, M., Barkmeijer, J., Dahlbom, M., Macpherson, B., Ballard, S., Inverarity, G., Carley, J., Alexander, C., Dowell, D., Liu, S., Ikuta, Y., and Fujita, T.: Survey of data assimilation methods for convective-scale numerical weather prediction at operational centres, Quarterly Journal of the Royal Meteorological Society, 144, 1218–1256, https://doi.org/10.1002/qj.3179, https://rmets.onlinelibrary.wiley.com/doi/abs/10.1002/qj.3179, 2018.

405 Gutman, S. I., Sahm, S. R., Benjamin, S. G., Schwartz, B. E., Holub, K. L., Stewart, J. Q., and Smith, T. L.: Rapid Retrieval and Assimilation
        of Ground Based GPS Precipitable Water Observations at the NOAA Forecast Systems Laboratory: Impact on Weather Forecasts, Journal
        of the Meteorological Society of Japan. Ser. II, 82, 351–360, https://doi.org/10.2151/jmsj.2004.351, 2004.

     Kouba,   J.   and   Héroux,   P.:   Precise   Point   Positioning   Using   IGS   Orbit   and   Clock   Products,   GPS   Solutions,
        https://doi.org/https://doi.org/10.1007/PL00012883, 2001.

410 Macpherson, S. R., Deblonde, G., Aparicio, J. M., and Casati, B.: Impact of NOAA Ground-Based GPS Observations on the Canadian
        Regional Analysis and Forecast System, Monthly Weather Review, 136, 2727–2746, https://doi.org/10.1175/2007MWR2263.1, https:
        //doi.org/10.1175/2007MWR2263.1, 2008.

     Mahfouf, J.-F., Ahmed, F., Moll, P., and Teferle, F. N.: Assimilation of zenith total delays in the AROME France convective scale model:
        a recent assessment, Tellus A: Dynamic Meteorology and Oceanography, 67, 26 106, https://doi.org/10.3402/tellusa.v67.26106, https:

415   //doi.org/10.3402/tellusa.v67.26106, 2015.

     Pinty, J.-P. and Jabouille, P.: A mixed-phased cloud parameterization for use in a mesoscale non-hydrostatic model: simulations of a squall
        line and of orographic precipitation. Proceeding, Conference on Cloud Physics, Everett, WA,, Amer. Meteor. Soc., pp. 217–220, 1998.

     Protat, A., Bouniol, D., Delanoë, J., O'Connor, E., May, P. T., Plana-Fattori, A., Hasson, A., Görsdorf, U., and Heymsfield, A. J.: Assess-
        ment of Cloudsat Reflectivity Measurements and Ice Cloud Properties Using Ground-Based and Airborne Cloud Radar Observations,

420   Journal of Atmospheric and Oceanic Technology, 26, 1717–1741, https://doi.org/10.1175/2009JTECHA1246.1, https://doi.org/10.1175/
        2009JTECHA1246.1, 2009.

     Ricard, D., Ducrocq, V., and Auger, L.: A Climatology of the Mesoscale Environment Associated with Heavily Precipitating Events over a
        Northwestern Mediterranean Area, J. Appl. Meteor. Climatol., 51, 468–488, 2012.

     Saïd, F., Campistron, B., Delbarre, H., Canut, G., Doerenbecher, A., Durand, P., Fourrié, N., Lambert, D., and Legain, D.: Offshore winds

425   obtained from a network of wind-profiler radars during HyMeX, Quarterly Journal of the Royal Meteorological Society, 142, 23–42,
        https://doi.org/10.1002/qj.2749, https://rmets.onlinelibrary.wiley.com/doi/abs/10.1002/qj.2749, 2016.

     Seity, Y., Brousseau, P., Malardel, S., Hello, G., Bénard, P., Bouttier, F., Lac, C., and Masson, V.: The AROME-France convective scale
        operational model., Mon.Wea.Rev., 139, 976–991, 2011.

     Wattrelot, E., Caumont, O., and Mahfouf, J.-F.: Operational Implementation of the 1D+3D-Var Assimilation Method of Radar Reflectivity

430   Data in the AROME Model, Monthly Weather Review, 142, 1852–1873, https://doi.org/10.1175/MWR-D-13-00230.1, https://doi.org/10.
        1175/MWR-D-13-00230.1, 2014.